Chemical Physics Letters 831 (2023) 140807

Contents lists available at ScienceDirect

Chemical Physics Letters

journal homepage: www.elsevier.com/locate/cplett

Research paper

Assessing the dipolar-octupolar NLO behavior of substituted thiosemicarbazone assemblies

Rodrigo Gester [a,b,*], Marcelo Siqueira [c], Antonio R. Cunha [d], Raiane S. Araújo [e], Patricio F. Provasi [f], Sylvio Canuto [b]

[a] Faculdade de Física, Universidade Federal do Sul e Sudeste do Pará, Marabá-, PA, 68507-590, Brazil
[b] Instituto de Física, Universidade de São Paulo, Rua do Matão 1371, São Paulo, SP 05588-090, Brazil
[c] Curso de Física, Universidade Federal do Amapá, 68903-329, Ramal da UNIFAP, Macapá, AP, Brazil
[d] Universidade Federal do Maranhão, UFMA, Campus Balsas, CEP 65800-000, Maranhão, Brazil
[e] Departamento de Física, Universidade Federal de Sergipe, 49100-000, São Cristóvão, SE, Brazil
[f] Department of Physics, IMIT, Northeastern University, CONICET, AV. Libertad 5500, W 3404 AAS Corrientes, Argentina

HIGHLIGHTS

- The NLO response of new thiosemicarbazone molecules is the first time assessed.
- The presence of Cl and Br causes a moderate redshift in the UV–Vis spectra.
- The simple substitution of H by Cl and Br atoms enhances the NLO behavior.
- Thiosemicarbazone molecules are intermediate octupolar ($\Phi_{J=3}$ = 70%) chromophores.
- Bromine atoms amplify the PDOS contributions of C rings and central atoms.

GRAPHICAL ABSTRACT

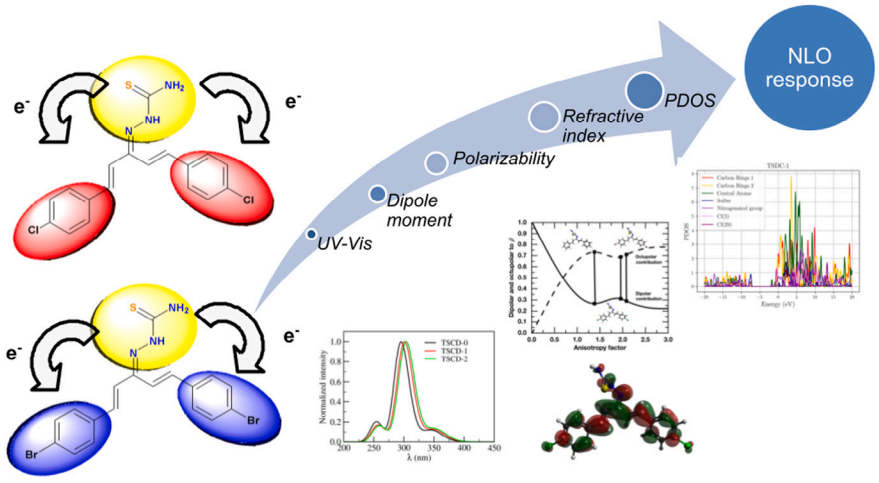

ARTICLE INFO

Keywords:
Nonlinear optics
Octupolar contributions
UV–vis spectra
Chlorine and bromine substitution
DFT methods

ABSTRACT

Density Functional Theory with hyper-Rayleigh scattering is used to investigate the non-linear optical response of newly synthesized thiosemicarbazone molecules. The systems present low refractive indices, and PDOS analyses indicate that the substituents chlorine and bromine induce a batchromism in the UV–Vis spectra and significantly improve (ca. 69%) the estimate of the first hyperpolarizability (β_{HRS}) to values fifty times higher than those reported for urea ($\beta = 0.34 \times 10^{-30}$ esu). Moreover, intramolecular charge transfer processes and evident octupolar contributions ($\Phi_{J=3} \approx 70\%$) account for the NLO behavior. The results suggest potential uses in optoelectronics and photonics.

* Corresponding author at: Faculdade de Física, Universidade Federal do Sul e Sudeste do Pará, Marabá-, PA, 68507-590, Brazil.
E-mail address: gester@unifesspa.edu.br (R. Gester).

https://doi.org/10.1016/j.cplett.2023.140807
Received 17 March 2023; Received in revised form 23 July 2023; Accepted 25 August 2023
Available online 6 September 2023

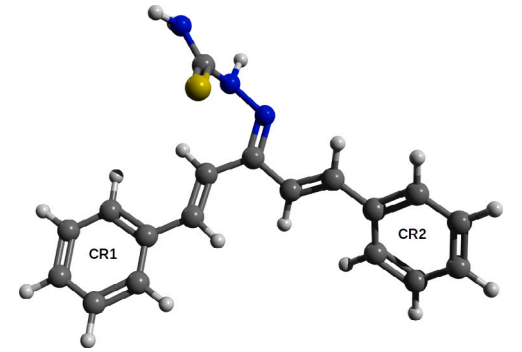

(a) TSCD-H

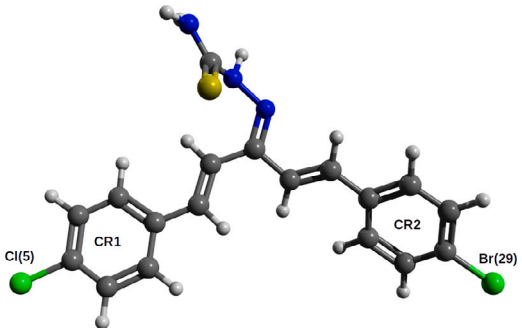

(b) TSCD-Cl

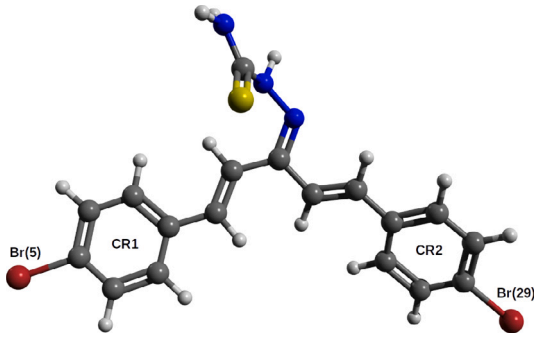

(c) TSCD-Br

Fig. 1. Optimized structures of thiosemicarbazone molecules. The chemical elements are colored, hydrogen (white), carbon (gray), nitrogen (blue), sulfur (yellow), chlorine (green), and bromine (brown).

1. Introduction

Nonlinear optical (NLO) materials are compounds capable of manipulating photonic signals efficiently, functionalizing various electro-optical circuits useful for tasks such as optical communication, computation, and dynamic image processing, for example. These devices are advantageous in that they transmit data information as fast as the speed of light in the medium allows. Thus, since the first observation of NLO effects, efforts have been made to discover new compounds with improved optical behavior.

In this race, organic dyes took the lead compared to inorganic chromophores, since these compounds present an expressive decomposition threshold against high-power lasers. Furthermore, its structure can be manipulated by standard chemical synthesis, which can incorporate anything from simple chemical elements to complete molecular structures. Therefore, various squaraine, azo dyes, and other chromophores have been proposed as chalcones mainly for NLO uses.

In previous work, one of us synthesized and characterized a variety of thiosemicarbazone derivatives (see Fig. 1), which have exhibited appreciable two-photon absorption properties [1,2], suggesting enhancement of NLO activity. These compounds differ from other proposals by the presence of the substituents, chlorine and bromine, which have shifted the absorption spectra of one-photon to lower energies. Although this effect sometimes indicates an enhancement of the NLO response of a chromophore, no effort has been made to verify and confirm this expectation.

In a scenario in which NLO experiments are costly and prohibitive, molecular modeling techniques are imposed since they can provide relevant preliminary information and elucidate aspects that are not yet clarified. Therefore, for the first time, we carried out a careful analysis of the Time-Dependent Density Functional Theory (TD-DFT) [3] together with the hyper-Rayleigh scattering (HRS) formalism [4] to investigate the second-harmonic generation procedure in said chromophores in gas conditions.

Additionally, two-photon absorption (2PA) is a third-order nonlinear optical process that plays an important role in nonlinear optical spectroscopy [5]. In this process, the material simultaneously absorbs two photons of identical frequencies, and the energy difference between the initial and final states corresponds to the sum of the energies of the two absorbed photons. The 2PA process has attracted great scientific interest, both from experimental and theoretical perspectives. Therefore, materials exhibiting high 2PA values have several relevant applications, such as the development of optical sensors [6], microfabrication [7], two-photon fluorescence imaging [8] and photodynamic therapy [9].

The main objective of this work is to understand how the presence of substituents, chlorine, and bromine, alters the electronic structure and therefore activates the optical behavior of these materials. To do this, we thoroughly analyze the low refractive index (n) and a first hyperpolarizability (β_{HRS}). In addition, we study the optical response of chlorine- and bromine-doped chromophores, intramolecular charge transfer (ICT) processes, and the octupolar ($\beta_{J=3}$) and dipolar ($\beta_{J=1}$) architectures, thus demonstrating the ability of these chromophores for NLO applications.

2. Methodology

The molecular geometries and vibrational frequencies of the isolated molecules were studied using the theoretical level B3LYP/6-31+G(d). As a standard, the absence of negative vibrational frequencies corroborated the existence of local minimum energy geometries.

With respect to NLO parameters, all results were obtained using the base-coupled exchange–correlation (M06-2X) DFT methods with the 6-311++G(d,p) basis set and within the HRS setup. The entire discussion is maintained around the frequency-dependent first hyperpolarizability (β_{HRS}). As for the contributions to β_{HRS}, as usual. The analysis was performed based on the depolarization ratio (DR), dipolar ($\beta_{J=1}$), and octupolar ($\beta_{J=3}$), as well as the NLO anisotropy ($\rho = |\beta_{J=3}|/|\beta_{J=1}|$), which defines the dipole $\left(\boldsymbol{\Phi}_{J=1} = \frac{1}{1+\rho}\right)$ and octupole $\left(\boldsymbol{\Phi}_{J=3} = \frac{\rho}{1+\rho}\right)$ contributions. This formalism is fully described in previous works [4]. In addition, we also analyze the 2PA cross-section ($\sigma_{2\mathrm{PA}}$), which is another NLO parameter [10].

Finally, although all the quantum mechanical calculations have been carried out in the Gaussian 09 [11] program, the complete analysis of the optical parameters has been carried out according to the Multiwfn code [12].

3. Results

3.1. UV–Vis spectra interpretation

Although the TSCD-H molecule has been synthesized and spectroscopically characterized prior to this work [1], no investigations are available on its UV–Vis spectra. However, Araújo et al. made an experimental discussion on the absorption spectra of the TSCD-Cl

Table 1
Absorption band and two-photon absorption.

(a) Photophysical description of the maximum absorption band obtained using the M06-2X/6-311++G(*d,p*) level of quantum mechanics.

Chromophore	No.	λ (nm)	O.S.	Major contributions
TSCD-H	1	305.88	0.233	H→L (42%)
	2	294.80	0.632	H-3→L (64%)
	3	289.00	0.259	H-2→L (75%)
TSCD-Cl	1	309.01	0.396	H→L (32%)
	2	299.52	0.640	H-3→L (49%)
	3	292.99	0.271	H-2→LUMO (67%)
TSCD-Br	1	310.30	0.533	H→L (26%)
	2	301.31	0.591	H-3→L (41%)
	3	294.62	0.262	H-2→L (63%)

(b) 2PA cross-section parameters for the first excited states of the investigated gas-phase systems using B3LYP/6-31+G[a] for all but Br (6-31G).

Molecule	n	E (eV)	σ (a.u.)	σ (GM)[a]
TSCD-H	1	2.84	2.51E+00	1.39
	2	3.03	1.17E+00	0.58
	3	3.60	6.77E+01	35.76
	4	3.62	1.85E+01	9.78
TSCD-Cl	1	2.77	3.05E+00	1.61
	2	2.98	1.31E+00	0.69
	3	3.52	7.04E+01	37.11
	4	3.53	7.25E+01	38.22
TSCD-Br	1	2.77	3.11E+00	0.52
	2	2.98	1.73E+00	0.91
	3	3.49	8.04E+01	42.88
	4	3.51	9.63E+01	50.77

[a] The conversion factor from atomic units (au) to GM is 1.896788.

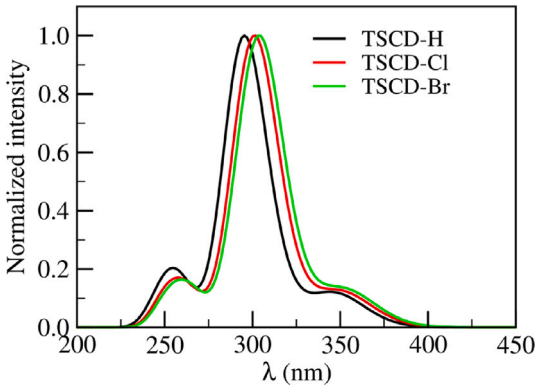

Fig. 2. Theoretical UV–Vis absorption spectra calculated for thiosemicarbazone using the time-dependent M06-2X/6-311++G(*d,p*) level of quantum mechanics.

and TSCD-Br molecules [2]. According to their results, between 250 and 400 nm there is a strong and pronounced absorption band. In addition, the experiment indicates a bathochromic change from the doped compounds to those synthesized with hydrogen atoms.

Due to the appreciable width of this band, it can be assumed that it is a region composed of several strong electronic excitations. To better understand the photophysics of the title chromophores, we performed an investigation with TD-DFT at M06-2X/6-311++G(*d,p*) level of quantum mechanics for isolated molecules, and the excitations performed in this spectral region are organized in Table 1.

For the original hydrogenated compound (TSCD-H), we found three close excitations that make up the main absorption band region. The lowest occurs at 305.9 nm with a corresponding oscillator strength of 0.23. This excitation corresponds to two transitions, H→L (42%) and H→L+5 (18%). However, the absorption maximum (λ_{max}) corresponds to an intense excitation located at 294.8 nm, which occurs in association with the strongest oscillator strength (0.63), being dominated mainly by the transitions H-3→L (64%) and H-2→L (11%). Finally, there is a last excitation at 289 nm due to the H-2→L transition (75%). Furthermore, analysis of these molecular orbitals also reveals $\pi \rightarrow \pi^*$ symmetry. We do not compare with experimental values because, to our knowledge, experimental λ_{max} values for TSCD-H are not available in the literature. However, for TSCD-Cl, these three excitations were estimated to be 309.0, 299.5, and 293.0 nm, and the oscillator forces presented similar values to those of TSCD-H. In the case of TSCD-Br, these three excitations were found in the same region of TSCD-Cl and best mapped to transitions H→L, H-3→L, and H-2→L, respectively. The experimental values of broadband λ_{max} with two peaks around ~300 nm and ~342 nm for TSCD-Cl and an absorption band with a peak around ~337 nm for TSCD-Br were reported by Araújo et al. [2]. For the main band, these experimental values agree with those obtained in the present investigation. The normalized intensities in the calculated spectrum shown in Fig. 2 also demonstrate a general agreement with the average experimental values. However, it is worth noting that accurately reproducing intensities can be more challenging.

From Table 1, the characteristics due to the substitution with Cl and Br, respectively, can be observed. First, all three thiosemicarbazones show the same electronic for up to the lowest absorption band. However, for TSCD-H and TSCD-Cl, a bathochromic shift is obtained ($\Delta\lambda = \lambda_{max}^{TSCD\text{-}Cl} - \lambda_{max}^{TSCD\text{-}H} \approx 5$ nm), as well as an increase in the intensity of absorption, as shown in Fig. 2. Bromine substitution produces a similar effect, but in this case, the electronic excitations are moved further towards lower energies, with $\Delta\lambda = \lambda_{max}^{TSCD\text{-}Br} - \lambda_{max}^{TSCD\text{-}H} \approx 7$ nm.

The bathochromic change caused by chlorine substitution has been reported for various other dyes. For example, Lokhande et al. [13,14] have synthesized a class of novel carbazole D-π-A chromophores with Cl in π-spacer, and in addition to improved NLO response, positive UV–Vis changes have been observed. Also recently, Jawaria et al. [15] demonstrated that the insertion of Cl and Br elements, in a stacking configuration in ferrocene-substituted thiosemicarbazone with triclinic crystal lattice, causes a redshift in the electronic transitions of compounds based on thiosemicarbazones.

3.2. Two-photon absorption cross-section analysis

After calculating the linear absorption parameters and the first hyperpolarizability, we calculate the 2PA properties of the first excited states in the gas phase of the investigated molecules. First, we calculate the tensor elements $S_{\alpha\beta}^{gf}$ that are best described in Ref [16].

From the theoretical results of σ_{2PA} obtained for the compounds TDSC-H, TSC-Cl, and TDSC-Br, we observe that they have values ranging from 35 GM to 50 GM in gas-phase, as shown in Table 1. Here, we observe that the TSCD-Br compound exhibited a higher σ_{2PA} value than TSCD-Cl, which differs slightly from what was observed experimentally. The TSCD-Cl and TSCD-Br compounds were previously reported in solvent media, specifically in dichloromethane (DCM), with maximum values of 69 GM and 66 GM, respectively. However, we firmly believe that this difference in values is directly related to the solvent effect since they are of the same order of magnitude. It is important to note that in our calculations we were able to predict two transitions close to the peak of the 2PA band, which was also observed experimentally. The authors performed a full scan of the 2PA band, indicating band overlap, although the contribution of each transition was not explicitly highlighted. Furthermore, it is important to highlight that the substitution by Br and Cl resulted in a slight increase in the 2PA values compared to the unsubstituted compounds, which is expected due to the strong donor character of the halogens [17].

Table 2
Permanent dipole moment (μ/D), dipole polarizability ($\alpha/10^{-24}$ esu), refractive index (n), frequency-dependent (ω = 1064 nm) first hyperpolarizability ($\beta/10^{-30}$ esu), energy-gap (E_g/eV), frontier molecular orbital energies ($E_{H/L}$/eV), dipolar ($\Phi_{J=1}$) and octupolar ($\Phi_{J=3}$) contributions, the nonlinear anisotropy (ρ) and depolarization (DR) ratios calculated at DFT/6-311++G(d,p) theory level.

Chromophore	Property	M06-2X	CAM-B3LYP	ωB97XD
TSCD-H	μ	3.338	3.403	3.429
	α_{iso}	42.560	42.972	42.801
	n	1.743	1.928	2.156
	β_{HRS}	9.140	9.697	9.138
	E_g	5.785	7.307	6.187
	E_H	−7.215	−7.835	−7.311
	E_L	−1.429	−0.528	−1.124
	$\lvert\beta_{J=1}\rvert$	9.438	10.576	9.663
	$\lvert\beta_{J=3}\rvert$	25.872	26.950	25.667
	$\Phi_{J=1}$	0.267	0.282	0.274
	$\Phi_{J=3}$	0.733	0.718	0.726
	ρ	2.741	2.548	2.656
	DR	2.040	2.118	2.073
TSCD-Cl	μ	3.919	3.927	3.983
	α_{iso}	47.879	48.125	47.922
	n	1.840	2.020	2.340
	β_{HRS}	15.461	15.820	14.720
	E_g	5.693	6.090	7.206
	E_H	−7.380	−7.476	−8.002
	E_L	−1.687	−1.386	−0.796
	$\lvert\beta_{J=1}\rvert$	18.627	19.499	17.884
	$\lvert\beta_{J=3}\rvert$	41.235	41.724	39.100
	$\Phi_{J=1}$	0.311	0.318	0.314
	$\Phi_{J=3}$	0.689	0.682	0.686
	ρ	2.214	2.140	2.186
	DR	2.298	2.347	2.316
TSCD-Br	μ	4.172	42.044	4.244
	α_{iso}	44.805	44.779	44.915
	n	1.803	1.803	1.739
	β_{HRS}	15.356	15.104	13.853
	E_g	5.709	6.115	7.218
	E_H	−7.136	−7.181	−7.765
	E_L	−1.428	−1.066	−0.547
	$\lvert\beta_{J=1}\rvert$	17.235	16.950	15.122
	$\lvert\beta_{J=3}\rvert$	42.225	41.534	38.489
	$\Phi_{J=1}$	0.290	0.290	0.282
	$\Phi_{J=3}$	0.710	0.710	0.718
	ρ	2.450	2.450	2.545
	DR	2.164	2.164	2.120
Urea	β_{HRS}	0.326	0.326	0.358
p-nitroaniline	β_{HRS}	6.418	6.663	6.450

3.3. Dipole moment, polarizability and refractive index

For different methods based on DFT, Table 2 show the calculated values for the permanent dipole moment (μ), the isotropic component of the dipole polarizability (α_{iso}) and the refraction index (n) calculated with the help of the Lorentz–Lorenz equation, $(n^2-1)/(n^2+2) = 4\pi\alpha_{iso}/3V_{mol}$ [18,19].

It can be seen that the main effect of substitution with chlorine and bromine is to monotonously increase μ. For TSCD-H to TSCD-Br molecules, the M06-2X method predicts a value of 3.338 D, which increases to 3.919 and 4.172 D respectively. The same pattern is observed for CAM-B3LYP and ωB97XDct.

The α_{iso} and n parameters, on the other hand, first increase from TSCD-H to TSCD-Cl in 5.319×10^{-24} esu and 0.097, but then decrease from TSCD-Cl to TSCD-Br in 3.074×10^{-24} esu and 0.037. Again the same pattern is observed for the other two functionals CAM-B3LYP and ωB97XD. In particular, n varies very little maintaining its value low and therefore making possible the use in conductive-light devices.

On the other hand, it is possible to connect the behavior of α_{iso} and n to the electronic structure of the material, providing a simple and complete understanding of the investigated phenomenon. The solution to the problem can be easily understood based on the HOMO (E_H) and LUMO (E_L) energies. It has been shown that the isotropic component of the dipole polarizability (α_{iso}) is a decreasing linear function of the chemical hardness ($\eta = E_g/2$) [20–22]. Also, since E_g(H) > E_g(Br) > E_g(H), one should get α_{iso}(H) < α_{iso}(Br) < α_{iso}(Cl), according to the results shown in Table 2. In the same way, according to the Moss relation, $n^4(E_g - 0.365) = 154$ [23], the refractive index must present the behavior regarding the energy gap. Also, n(H) < n(Br) < n(Cl), as shown in Table 2.

3.4. First hyper-polarizability analysis

The bathochromic shift of electronic transitions is an indicator of NLO enhancement. The existence of a linear relationship between the first hyperpolarizability and the absorption maxima ($\beta \propto \lambda_{max}$) is known, either for dipolar or octupolar NLO compounds [24–27]. For the particular case of the title compounds, current quantum mechanical calculations confirm the validity of this relationship. As can be seen, Table 2 presents the NLO results in the gas phase considering different degrees of exchange–correlation functionals. Among the chromophores investigated, the TSCD-H dye presents the lowest NLO response. For example, the results of M06-2X indicate that the first hyperpolarizability is of 9.140×10^{-30} esu. The CAM-B3LYP and ωB97XD functionals confirm it report values of 9.697×10^{-30} and $9,138\times10^{-30}$ esu respectively.

The first hyperpolarizabilities increase considerably when substituting hydrogen with chlorine in TSCD-Cl, *i.e.* an increase of 6.321×10^{30} esu, approx. 70% more than TSCD-H, but then substituting chorine by bromine in TSCD-Br, there is a slight decrease with respect to TSCS-Cl of $\sim0.1\times10^{30}$ esu, *i.e.* there is almost no change. Furthermore, the other DFT methods (CAM-B3LYP and ωB97XD) almost repeat the same pattern.

Unfortunately, experimental results for the optical activity of TSCD molecules are not yet available. However, molecular modeling techniques associated with quantum chemical approximations allow a comparison with other standard NLO materials. For instance, our M06-2X/6-311++G(d,p) performed in gas-phase urea reveals a frequency-dependent hyperpolarizability of 0.325×10^{30} esu. For different solvent environments, other reports have estimated values around 0.34×10^{30} esu [28,29]. Thus, it is noted that the predicted values for the TSCD molecules are between 28 and 48 times higher than those estimated for urea.

However, it can be considered unfair to compare it with urea due to its small size. But regarding *p*-nitroaniline, which is another NLO dye with interesting two-photon absorption properties [10], our M06-2X/6-311++G(d,p) calculations indicate a value of 6.42×10^{-30} esu for the β_{HRS} of the isolated molecule. Other theoretical reports have estimated values between 6.27×10^{-30} and 8.86×10^{-30} esu in different environments [30]. In any case, these values stand modest when compared to the results obtained for the TSCD derivatives.

Due to the experimental simplicity of obtaining the absorption spectra of one-photon, it is usual to apply the linear relation $\beta \propto \lambda_{max}$ as a first indication of the NLO response of a material. However, as Oudar and Chemla have shown for dipolar NLO chromophores, and Zyss et al. [24–26] have done the same for octupolar compounds, an inverse relationship can be established between the first hyperpolarizability and the excitation energy, ($\Delta\beta \propto 1/\Delta E$), allowing to connect of the NLO parameters and the electronic structure of the material [20,31–33]. Therefore, structural changes or intermolecular interactions due to the chromophore and the environment that decreases the energy gap would lead to a higher NLO response. This statement has been extensively discussed and used to clarify the optical knowledge of the material in several works as [34–40].

Concerning the molecular eigenstates, when HOMO and LUMO populate different molecular sites, HOMO-LUMO excitation occurs with considerable difficulty, in contrast to that situation where there is an overlap between these molecular eigenstates. From Fig. 3, it can be seen that the HOMO and LUMO of all the molecules present similar

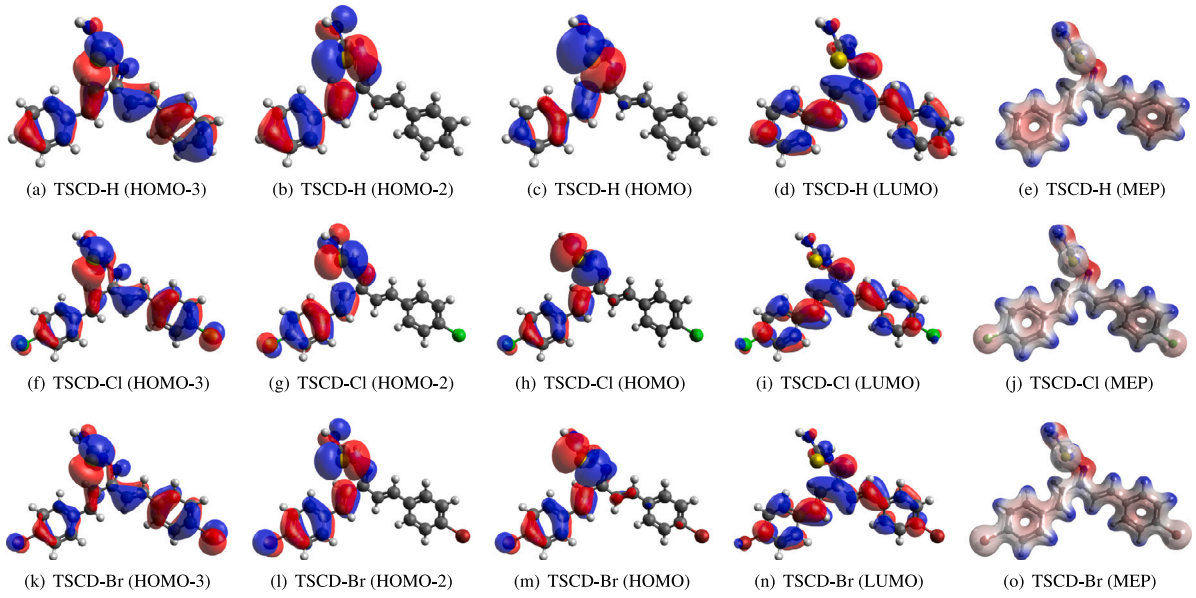

Fig. 3. The Kohn–Sham molecular orbitals are involved in the dominant electronic excitations of TSCD-H (top line), TSCD-Cl (middle line), and TSCD-Bd (bottom line). In the last column, one can analyze the molecular electronic potential (MEP) diagram plot. As a standard for MEP charts, blue designates positive electrical charges, and red assigns negative charge densities. These surfaces were generated under the quantum mechanical level M06-2X/6-311++G(*d*,*p*).

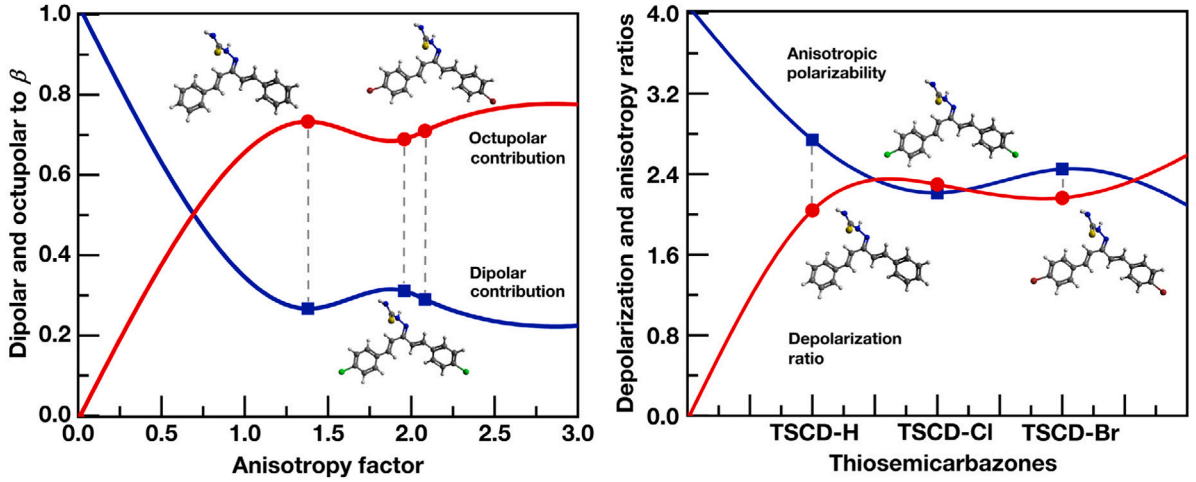

Fig. 4. On the left side is the evolution of the dipolar ($\Phi_{J=1}$) and octupolar ($\Phi_{J=3}$) contributions to the first hyperpolarizability. On the right side, the behavior of the anisotropy (ρ) and depolarization (DR) relationships are shown.

symmetry and topology. Therefore, the justification for the increase in the optical response of TSCD-0 to chlorine and bromine derivatives is not in the shape and location of the molecular orbitals but in their eigenvalues. For example, based on the results of M06-2X, from TSCD-H to TSCD-Cl, the energy gap decreases from 5.785 to 5.693 eV, facilitating the electronic transition and the NLO response [24].

Furthermore, the topology of the frontier molecular orbitals indicates that there is an intramolecular charge transfer (ICT) from the nitrogenous group to the ring on the right-hand side, and Fig. 5 better explains the central idea of this transfer. On the other hand, the molecular electrostatic potential mapping performed in Fig. 3 shows that the presence of the substituents Chlorine and Bromine accentuates the ICT process. The blue and red colors indicate the number of positive and negative charges, respectively. From TSCD-H to the other chromophores, an increase in electron density is noted around the chlorine and bromine sites. This procedure, of course, is a three-dimensional effect and has relevant implications for the NLO phenomenon.

However, suppose an ICT procedure only based on the HOMO-LUMO topology is dangerous. Therefore, one can corroborate this effect by comparing the electronic charges and dipole moment of the ground and the first excited states (GE and ES) calculated without relaxing the excited state geometry. This simple analysis would be enough to confirm an ICT regime. As an example, M06-2X/6-311++G(*d*,*p*) calculations performed at gas-phase indicate $\mu_{ES} > \mu_{GS}$. For TSCD-H, $\Delta\mu = \mu_{ES} - \mu_{GS} = 2.05$ D, and for the remaining chromophores, this variation is even greater, with $\Delta\mu^{Cl} = 3.82$ D and $\Delta\mu^{Br} = 3.81$ D, respectively. Moreover, after computing the electronic charges in the molecular region covered by the yellow surface shown in Fig. 5, we obtained $\Delta Q = Q_{ES} - Q_{GE} > 0$, proving that this region loses electrons that migrate to the other molecular region. Precisely, we obtained $\Delta Q^{H} = 0.244e$, $\Delta Q^{Cl} = 0.233e$, and $\Delta Q^{Br} = 0.249e$. Furthermore, the ICT procedure for TSCD molecules is a reality.

3.5. Dipolar and octupolar contributions

Normally, one can separate the NLO activity of a chromophore into dipolar ($\Phi_{J=1}$) and octupolar ($\Phi_{J=3}$) contributions [24]. Dipole characteristics prevail in cases where ICTs are almost one-dimensional

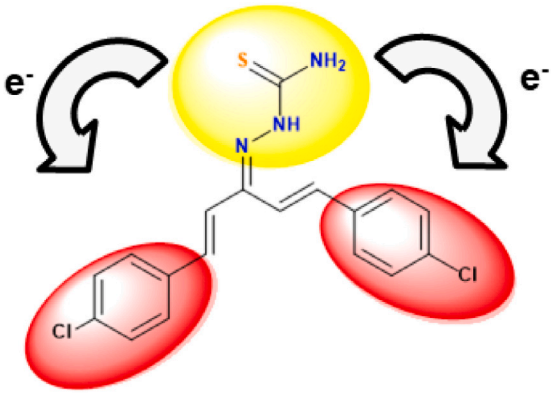

Fig. 5. Scheme of the internal charge transfer (ICT) process that occurs for thiosemicarbazone molecules from the yellow to the red surface. From the ground to the first excited state without relaxing the molecular geometries, the variation of the Mulliken charges on the yellow surface is $\Delta Q_{\mathrm{H}} = 0.244e$, $\Delta Q_{\mathrm{Cl}} = 0.233e$, and $\Delta Q_{\mathrm{Br}} = 0.2249e$, indicating charge migration to the surface in red.

and are well understood by two-level models, such as the one proposed by Oudar and Chemla [41]. However, the limits of such approximations are known and well discussed by Zyss and coworkers [25,26,42–44]. For trigonal systems, especially those with D_3h symmetry, the ICT procedure becomes three-dimensional and two-level models become ineffective. Therefore, approximations of three- [42] or even five-levels [43,44] are necessary.

Although Table 2 shows all the data needed to discuss dipolar-octupolar characteristics, Fig. 4 might provide a better visualization of the results. With $\Phi_{J=3} \approx 70\%$, it can be seen that all TSCD chromophores are defined as octupolar systems. However, as discussed above, the substituents chlorine and bromine slightly increase the dipolar character. For example, from TSCD-H to TSCD-Cl, $\Phi_{J=1}$ increases from 26.7 to 31.1%. This characteristic is caused by variations in the dipole moment, which augments from 3.338 D (TSCD-H) to 3.919 D (TSCD-Cl) and forces the ICT procedure to be closer to a one-dimension, preferably in the μ direction.

Furthermore, by scanning the anisotropic polarizability (ρ) and the depolarization ratio (DR), the degree of octupolarity of the system can be determined. In particular, ρ determines that a chromophore is completely dipolar or octupolar if $\rho \to 0$ or $\rho \to \infty$, respectively. Thus, with values ranging from 2.741 to 2.214, the anisotropic polarizability classifies all TSCD derivatives as octupolar compounds. On the other hand, DR can oscillate between values between 1.5 (octupolar) and 9 (dipolar). In the particular case of the title compounds, DR is between 2.040 and 2.164 *i.e.* confirm the octupolarity of the TSCD derivatives.

Concerning the classification, some scales propose to group the molecular systems according to the octupolarity scale. One of them is the classification proposed by Zhang et al. [4]. According to these proposals, the TSCD molecules would be intermediate octupolar compounds. Even though these molecular systems have no symmetry, or what is the same they all have a C_1 symmetry, at a glance, it can be noted that they are not too far from a D_{2h}, hence the importance of the octupolar character, in the studied molecular systems, is in agreement with this fact [24].

3.6. PDOS interpretation

To better understand the electronic properties of TSDC derivatives and the specific effect of chlorine and bromine substituents, the Projected Density of States (PDOS) was calculated (see Fig. 6). Related to UV–Vis spectroscopy, PDOS is helpful for looking at which atomic or molecular orbitals, and consequently which atoms are involved in an electronic transition [45–48]. For TSDC-H, the PDOS was divided

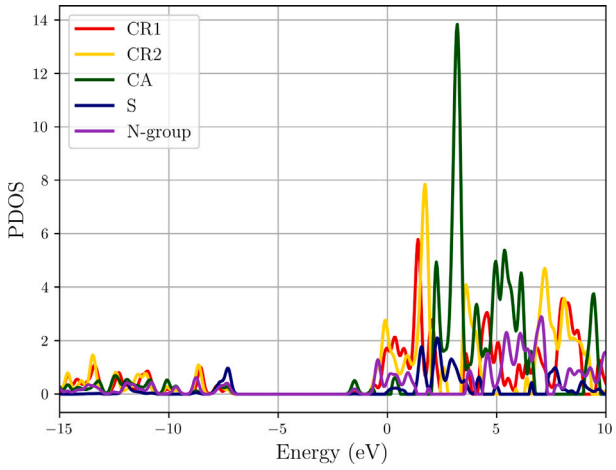

(a) TSCD-H

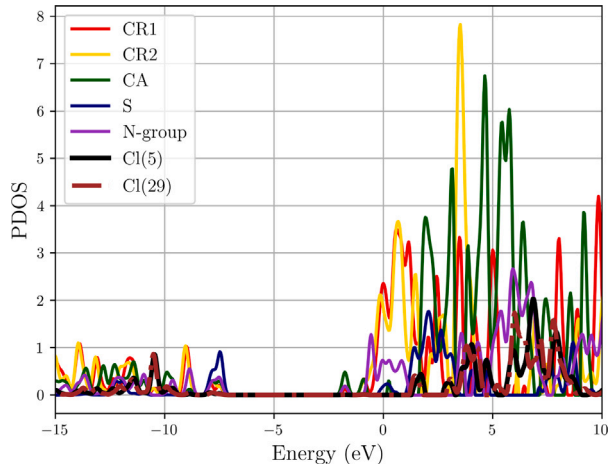

(b) TSCD-Cl

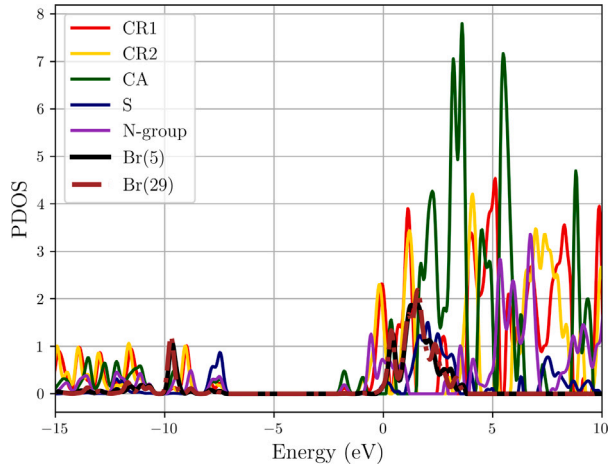

(c) TSCD-Br

Fig. 6. The PDOS of the TSDC-H molecule was divided into five groups: Carbon Ring 1 (CR1) in red, Carbon Ring 2 (CR-2) in gold, Central Atoms (CA) in dark green, Sulfur (S) in navy blue and Nitrogenated group (N-group) in dark orchid. For TSDC-Cl, the Cl atoms were placed at positions 5 and 29 (Cl(5) (Black) and Cl(29) (brown)). For TSDC-Br, the atoms at positions 5 and 29 are Br (Br(5) (black) and Br(29) (brown)).

into five components: Carbon Rings 1 (CR1) (on the left of Fig. 1a), Carbon Rings 2 (CR2) (on the right of Fig. 1a), central atoms (CA), S atom and N group (chain with three N atoms, the double bond between the C and S and H atoms) (see Fig. 1a). For TSDC-Cl, the H atoms at the farthest from the center of the molecule were exchanged for Cl, giving the extra Cl(5) and Cl(29) components to PDOS (see Figs. 1b and 6b). In the TSDC-Br derivative, these additional groups are occupied by Br atoms (Br(1) and Br(2)), as can be seen in Figs. 1c and 6c. Regarding the NLO response, the contribution of different molecular orbitals varies with the molecule's electronic structure. The relationship between hyperpolarizability and absorption maxima ($\beta \propto \lambda_{max}$) is directly affected since the presence of different dopants redistributes the atomic orbitals [24,25,27].

The PDOS of TSDC-H is shown in Fig. 6a. The CR1, CR2 and the N group dominate the region of occupied orbitals (−20.0 eV to −7.5 eV), but for HOMO (~7.5 eV), the most relevant contribution, comes from the sulfur atom, according to Fig. 3a (HOMO of the TSDC-H molecule). Comparing these data with the UV–Vis spectrum, the lowest absorption line has two excitations (see Table 1), one at 351.15 nm (3.53 eV), composed of CA, CR1, CR2, and S, and the other at 337.933 nm (3.67 eV) where CA begins to dominate, followed by the S atom. The three excitations with maximum absorption are composed of a peak at 305.88 nm (4.05 eV) that is almost completely dominated by CA, with minor contributions from CR1, CR2, and the S atom giving rise to an N-group. The second transition occurs at 294.8 nm (4.20 eV) and is a weaker combination of CR1, CR2, CA, and N-group. This transition corresponds to the strongest oscillator strength (0.6319). The last transition at 289.00 nm (4.29 eV) has the same combination of components, but the CA contributions are reduced and rise in intensity, equivalent to CR1 and CR2. The N-group does not change appreciably. Contributions beyond this range are outside the visible spectrum and are composed of CR1, CR2, CA, and N-group. The S has no appreciable peaks.

Fig. 6b describes the PDOS of TSDC-Cl. Compared to TSDC-H, it is observed at first sight the shift to higher energies of all PDOS peaks of the already seen molecular groups and the contributions coming from the Cl(5) and Cl(29) lines. In the region of occupied orbitals, there are no appreciable changes, but there is the aforementioned increase in the peaks. Compared to the UV–Vis spectrum, the lowest absorption line and its two transitions are recomposed (see Table 1). In the first, at 355.56 nm (3.49 eV), composed of CR1, CR2, CA, and group N, the presence of Cl(5) and Cl(29) is observed, which reduces the intensity of the CA bands and redistribute their strongest peak, giving rise to the highest peak of CR2 and minor contributions from CR1. In the second, at 341.41 nm (3.63 eV), the states are still dominated by CA, but the associated peak is weaker. CR1, S, Cl(5), and Cl(29) have important contributions, in this order. The band of maximum absorption, composed of transitions at 309.01 nm (4.01 eV), 299.52 nm (4.14 eV), and 292.99 nm (4.23 eV), sees its composition drastically affected. Compared with TSDC-H PDOS, it can be seen that the PDOS contributions are not dominated by CA, but are distributed in a band where CR2 has the dominant peak, followed by CA and has relevant contributions from CR1, group N, Cl(5), and Cl(29). Due to the relationship $\beta \propto \lambda_{max}$, this new composition of orbitals changes the hyperpolarizability, since there is a bathochromic change caused by chlorine insertion. Beyond this interval, there is a more equal distribution of orbitals, with the strongest contributions from CR1, CA, and CR2, respectively.

The PDOS of TSDC-Br, with Br atoms at positions 5 and 29 (Br(5) and Br(29)), is shown in Fig. 6c. It is possible to observe the shift to higher energies of the peaks in the whole spectrum, as it is observed for the Cl atoms. These results are coherent since the Cl and Br atoms have more electronic states than the H atoms. The bands related to CA are the most affected and wider bands and a strong separation of peaks can be seen in the region of the virtual states. Regarding the composition of molecular regions in the states available for transition, this molecule is closer to the description of TSDC-H. However, the Br bands are more intense in the visible region compared to the Cl bands. The lowest absorption band and its two peaks at 357.53 nm (3.47 eV) and 342.78 nm (3.62 eV) have major contributions provided by CA, followed by S atoms, N group, and Br. The band transitions of maximum absorption are 310.30 nm (4.00 eV), 301.31 nm (4.11 eV), and 294.62 nm (4.21 eV). The transitions are mainly composed of CR1, CR2, and CA. Other groups do not have appreciable participation, but Br(5) with a weaker peak in this interval. This composition of orbitals gives a small shift in λ_{max} compared to the TSDC-Cl results, but the most prominent effect observed due to the composition of the partial contributions comes from TSDC-Cl.

These results indicate that in these configurations the Cl atoms have a greater potential to change the partial contributions in the PDOS, but the Br atoms provide important changes in the optical response, due to the amplification of the CA contributions and the separation of their respective peaks.

4. Conclusions

Based on the TD-DFT within the HRS formalism and paying special attention to the doping of thiosemicarbazone with chlorine and bromine, we have carried out a systematic investigation of the optical response of these three recently synthesized derivatives. The substitution increases all the electrical properties. Although the refractive index increases as well, it still remains low, making these derivatives interesting for light conduction. The single-photon absorption spectra show an evident bathochromic shift, suggesting an enhancement of the nonlinear optical response with the substituent. This expectation was confirmed by analyzing the behavior of the first frequency-dependent hyperpolarizability, which especially for the doped chromophores showed a higher NLO response compared to standard materials such as urea, *p*-nitroaniline, and other dyes. Regarding the contributions to the NLO response, the results indicate an intermediate octupolar response, which dominates the optical phenomenon. Moreover, the calculated two-photon absorption spectra aligns previous experimental results, and reveals that the solvent has little influence on this NLO property. This agreement transmits confiability to the current NLO estimatives. After evaluating all the data, clear, the substituted thiosemicarbazone may be functional in NLO applications.

CRediT authorship contribution statement

Rodrigo Gester: Molecular modeling, Quantum chemical calculations, Analysis of the results and manuscript preparation. **Marcelo Siqueira:** Analysis of the results and manuscript preparation. **Antonio R. Cunha:** Analysis of the results and manuscript preparation. **Raiane S. Araújo:** Analysis of the results and manuscript preparation. **Patricio F. Provasi:** Molecular modeling, Quantum chemical calculations, Analysis of the results and manuscript preparation. **Sylvio Canuto:** Analysis of the results and manuscript preparation.

Declaration of competing interest

The authors declare that they have no known competing financial interests or personal relationships that could have appeared to influence the work reported in this paper.

Data availability

No data was used for the research described in the article

Acknowledgments

This study is financed in part by the Coordenação de Aperfeiçoamento de Pessoal de Nível Superior - Brasil (CAPES), Conselho Nacional de Desenvolvimento Científico e Tecnologico (CNPq), and Fundação de Amazônica de Amparo a Estudos e Pesquisas (FAPESPA). P.F.P. acknowledges financial support from CONICET (PIP: KE3-11220200100467CO).

References

[1] A.A. da Silva, P.I.S. Maia, C.D. Lopes, S. Albuquerque, M.S. Valle, Synthesis, characterization and antichagasic evaluation of thiosemicarbazones prepared from chalcones and dibenzalacetones, J. Mol. Struct. 1232 (2021) 130014, http://dx.doi.org/10.1016/j.molstruc.2021.130014.

[2] R.S. Araújo, L.F. Sciuti, L.H.Z. Cocca, T.O. Lopes, A.A. Silva, L.M.G. Abegão, M.S. Valle, J.J. Rodrigues Jr., C.R. Mendonça, L. De Boni, M.A.R.C. Alencar, Comparing two-photon absorption of chalcone, dibenzylideneacetone and thiosemicarbazone derivatives, Opt. Mater. 137 (2023) 113510, http://dx.doi.org/10.1016/j.optmat.2023.113510.

[3] C. Adamo, D. Jacquemin, The calculations of excited-state properties with time-dependent density functional theory, Chem. Soc. Rev. 42 (2013) 845, http://dx.doi.org/10.1039/c2cs35394f.

[4] L. Zhang, D. Qi, L. Zhao, C. Chen, Y. Bian, W. Li, Density functional theory study on subtriazaporphyrin derivatives: dipolar/octupolar contribution to the second-order nonlinear optical activity, J. Phys. Chem. A 116 (2012) 10249, http://dx.doi.org/10.1021/jp3079293.

[5] R.W. Boyd (Ed.), Nonlinear Optics, third ed., 2008.

[6] S. Pascal, S. David, C. Andraud, O. Maury, Near-infrared dyes for two-photon absorption in the short-wavelength infrared: strategies towards optical power limiting, Chem. Soc. Rev. (2021).

[7] M. Farsari, B.N. Chichkov, Two-photon fabrication, Nat. Photon. 3 (2009) 450, http://dx.doi.org/10.1038/nphoton.2009.131.

[8] L. Chen, M. Chen, Y. Zhou, C. Ye, R. Liu, NIR photosensitizer for two-photon fluorescent imaging and photodynamic therapy of tumor, Front. Chem. 9 (2021) 1, http://dx.doi.org/10.3389/fchem.2021.629062.

[9] T. Zhang, L. Fu, X. Zheng, M. Liu, Q. Pei, X. Wang, S. Liu, Two-photon excited organic nanoparticles for chemo-photodynamic therapy, Dye Pigment 167 (2019) 195, http://dx.doi.org/10.1016/j.dyepig.2019.04.038.

[10] T.N. Ramos, D.L. Silva, B.J.C. Cabral, S. Canuto, On the spectral line width broadening for simulation of the two-photon absorption cross-section of para-nitroaniline in liquid environment, J. Mol. Liq. 301 (2020) 112405, http://dx.doi.org/10.1016/j.molliq.2019.112405.

[11] M.J. Frisch, et al., Gaussian 09, Revision a.02, Gaussian Inc, Wallingford CT, 2016.

[12] T. Lu, F. Chen, Multiwfn: A multifunctional wavefunction analyzer, J. Comput. Chem. 33 (2012) 580, http://dx.doi.org/10.1002/jcc.22885.

[13] P.K.M. Lokhande, D.S. Patil, N. Sekar, Viscosity sensitive red shifted novel D-π-A carbazole chromophore with chlorine in π-spacer: Synthesis, photophysical properties, NLO study and DFT approach, J. Lumin. 211 (2019) 162, http://dx.doi.org/10.1016/j.jlumin.2019.03.028.

[14] P.K.M. Lokhande, D.S. Patil, M. Kadam, N. Sekar, Chlorine (Cl) - substituted carbazole based A-Π-D-Π-a push-pull chromophores as aggregation enhanced emission (AEE) active viscosity sensors: Synthesis, DFT and NLO approach, J. Fluoresc. 29 (2019) 779, http://dx.doi.org/10.1007/s10895-019-02396-y.

[15] R. Jawaria, M. Hussain, M. Khalid, M.U. Khan, M. Nawaz Tahir, M.M. Naseer, A.A.C. Braga, Z. Shafiq, Synthesis, crystal structure analysis, spectral characterization and nonlinear optical exploration of potent thiosemicarbazones based compounds: A DFT refine experimental study, Inorg. Chim. Acta 486 (2019) 162, http://dx.doi.org/10.1016/j.ica.2018.10.035.

[16] D.L. da Silva, L. De Boni, D.S. Correa, S.C.S. Costa, A.A. Hidalgo, S.C. Zílio, S. Canuto, C.R. Mendonça, Two-photon absorption in oxazole derivatives: An experimental and quantum chemical study, Opt. Mater. (Amst). 34 (2012) 1013, http://dx.doi.org/10.1016/j.optmat.2011.12.009.

[17] N.S.K. Reddy, R. Badam, R. Sattibabu, M. Molli, V.S. Muthukumar, S.S.S. Sai, G.N. Rao, Synthesis, characterization and nonlinear optical properties of symmetrically substituted dibenzylideneacetone derivatives, Chem. Phys. Lett. 616–617 (2014) 142, http://dx.doi.org/10.1016/j.cplett.2014.10.043.

[18] L. Lorenz, Ueber die refractions constante, Ann. Phys.-Berl. 247 (1880) 70, http://dx.doi.org/10.1002/andp.18802470905.

[19] H.A. Lorentz, Ueber die beziehung zwischen der fortpflanzungsgeschwindigkeit des lichtes und der körperdichte, Ann. Phys.-Berl. 245 (1880) 641, http://dx.doi.org/10.1002/andp.18802450406.

[20] R. Gester, A. Torres, A.R. da Cunha, T. Andrade-Filho, V. Manzoni, Theoretical study of thieno[3, 4-b]pyrazine derivatives with enhanced NLO response, Chem. Phys. Lett. 781 (2021) 138976, http://dx.doi.org/10.1016/j.cplett.2021.138976.

[21] K.R.S. Chandrakumar, T. Ghanty, S. Ghosh, Relationship between ionization potential, polarizability, and softness: A case study of lithium and sodium metal clusters, J. Phys. Chem. A 108 (32) (2004) 6661, http://dx.doi.org/10.1021/jp048522e.

[22] K. Gupta, T.K. Ghanty, S.K. Ghosh, Polarizability, ionization potential, and softness of water and methanol clusters: An interrelation, J. Phys. Chem. A 116 (2012) 6831, http://dx.doi.org/10.1021/jp3048357.

[23] R.R. Reddy, Y.N. Ahammed, Relation between energy gap and electronic polarizability of ternary chalcopyrites, Infrared Phys. Technol. 37 (1996) 505, http://dx.doi.org/10.1016/1350-4495(95)00073-9.

[24] D.R. Kanis, M.A. Ratner, J.T. Marks, Design and construction of molecular assemblies with large second-order optical nonlinearities, quantum chemical aspects, Chem. Rev. 94 (1994) 195, http://dx.doi.org/10.1021/cr00025a007.

[25] L.T. Cheng, W. Tam, S.H. Stevenson, G.R. Meredith, G. Rikken, S.R. Marder, Experimental investigations of organic molecular nonlinear optical polarizabilities, 1. Methods and results on benzene and stilbene derivatives, J. Phys. Chem. 95 (1991) 10631, http://dx.doi.org/10.1021/j100179a026.

[26] D.M. Burland, J.E. Rice, M. Stähelin, Molecular systems for nonlinear optical applications, Mol. Cryst. Liq. Cryst. Sci. Technol. 216 (2006) 27, http://dx.doi.org/10.1080/10587259208028744.

[27] R. Gester, A. Torres, C. Bistafa, R.S. Araújo, T.A. da Silva, V. Manzoni, Theoretical study of a recently synthesized azo dyes useful for OLEDs, Mat. Lett. 280 (2020) 128535, http://dx.doi.org/10.1016/j.matlet.2020.128535.

[28] M.J. Alam, A.U. Khan, M. Alam, S. Ahmad, Spectroscopic (FTIR, FT-raman, ^{1}h NMR and UV–vis) and DFT/TD-DFT studies on cholesteno [4, 6-b, c]-2, 5-dihydro-1, 5-benzothiazepine, J. Mol. Struct. 1178 (2019) 570, http://dx.doi.org/10.1016/j.molstruc.2018.10.063.

[29] A.K. Mishra, S.P. Tewari, Density functional theory calculations of spectral, NLO, reactivity, NBO properties and docking study of vincosamide-n-oxide active against lung cancer cell lines H1299, SN Appl. Sci. 2 (2020) 1021, http://dx.doi.org/10.1007/s42452-020-2842-9.

[30] S. Muhammad, A.G. Al-Sehemi, Z. Su, H. Xu, A. Irfan, A.R. Chaudhry, First principles study for the key electronic, optical and nonlinear optical properties of novel donor–acceptor chalcones, J. Mol. Graph. Model. 72 (2017) 58, http://dx.doi.org/10.1016/j.jmgm.2016.12.009.

[31] J.E.C. Águila, M. Trejo-Durán, Theoretical study of the second-order nonlinear optical properties of ionic liquids, J. Mol. Liq. 269 (2018) 833, http://dx.doi.org/10.1016/j.molliq.2018.08.057.

[32] A. Raiol, A.R. da Cunha, V. Manzoni, T. Andrade-Filho, R. Gester, Solvent enhancement and isomeric effects on the NLO properties of a photoinduced cis-trans azomethine chromophore: A sequential MC/QM study, J. Mol. Liq. 340 (2021) 116887, http://dx.doi.org/10.1016/j.molliq.2021.116887.

[33] Â.C.M. Pimenta, T. Andrade-Filho, V. Manzoni, J. Del Nero, R. Gester, Giant values obtained for first hyperpolarizabilities of methyl orange: a DFT investigation, Theor. Chem. Account. 138 (2019) 27, http://dx.doi.org/10.1007/s00214-018-2406-x.

[34] B. Baroudi, K. Argoub, D. Hadji, A.M. Benkouider, K. Toubal, A. Yahiaoui, A. Djafri, Synthesis and DFT calculations of linear and nonlinear optical responses of novel 2-thioxo-3-N, (4-methylphenyl) thiazolidine-4 one, J. Sulfur Chem. 41 (2020) 310, http://dx.doi.org/10.1080/17415993.2020.1736073.

[35] A. Merouane, A. Mostefai, D. Hadji, A. Rahmouni, M. Bouchekara, A. Ramdani, S. Taleb, Theoretical insights into the static chemical reactivity and NLO properties of some conjugated carbonyl compounds: case of 5-aminopenta-2, 4-dienal derivatives, Monatshefte Chem. - Chem. Mon. 151 (2020) 1095, http://dx.doi.org/10.1007/s00706-020-02653-y.

[36] D. Hadji, A. Rahmouni, D. Hammoutène, O. Zekri, First theoretical study of linear and nonlinear optical properties of diphenyl ferrocenyl butene derivatives, J. Mol. Liq. 286 (2019) 110939, http://dx.doi.org/10.1016/j.molliq.2019.110939.

[37] D. Hadji, B. Haddad, S.A. Brandán, S.K. Panja, A. Paolone, M. Drai, D. Villemin, S. Bresson, M. Rahmouni, Synthesis, NMR, Raman, thermal and nonlinear optical properties of dicationic ionic liquids from experimental and theoretical studies, J. Mol. Struct. 1220 (2020) 128713, http://dx.doi.org/10.1016/j.molstruc.2020.128713.

[38] D. Hadji, H. Brahim, Structural, optical and nonlinear optical properties and TD-DFT analysis of heteroleptic bis-cyclometalated iridium(III) complex containing 2-phenylpyridine and picolinate ligands, Theor. Chem. Accounts 137 (2018) 180, http://dx.doi.org/10.1007/s00214-018-2396-8.

[39] M. Boukabene, H. Brahim, D. Hadji, A. Guendouzi, Theoretical study of geometric, optical, nonlinear optical, UV–Vis spectra and phosphorescence properties of iridium(III) complexes based on 5-nitro-2-(2', 4'-difluorophenyl)pyridyl, Theor. Chem. Accounts 139 (2020) 47, http://dx.doi.org/10.1007/s00214-020-2560-9.

[40] D. Hadji, A. Rahmouni, Theoretical study of nonlinear optical properties of some azoic dyes, Mediterr. J. Chem. 4 (2015) 185, http://dx.doi.org/10.13171/mjc.4.4.2015.15.07.22.50/hadji.

[41] J.L. Oudar, D.S. Chemla, Hyperpolarizabilities of the nitroanilines and their relations to the excited state dipole moment, J. Chem. Phys. 66 (1977) 2664, http://dx.doi.org/10.1063/1.434213.

[42] J. Zyss, S. Brasselet, Multipolar symmetry patterns in molecular nonlinear optics, J. Nonlinear Opt. Phys. 07 (1998) 397, http://dx.doi.org/10.1142/S0218863598000302.

[43] M. Cho, Sun-Young. An, H. Lee, I. Ledoux, J. Zyss, Nonlinear optical properties of tetrahedral donor–acceptor octupolar molecules: Effective five-state model approach, J. Chem. Phys. 116 (2002) 9165, http://dx.doi.org/10.1063/1.1473818.

[44] S. Bidault, S. Brasselet, J. Zyss, Role of spatial distortions on the quadratic nonlinear optical properties of octupolar organic and metallo-organic molecules, J. Chem. Phys. 126 (2007) 034312, http://dx.doi.org/10.1063/1.2428308.

[45] L. Zhang, K. Xu, Understanding substitution effects on dye structures and optoelectronic properties of molecular halide perovskite Cs 4 MX 6 (M=Pb Sn, Ge; X= Br, I, Cl), J. Mol. Graph. Model. 91 (2019) 172, http://dx.doi.org/10.1016/j.jmgm.2019.06.009.

[46] D.F. Ferreira, W.D. Oliveira, E. Belo, R. R. Gester, M.R. Siqueira, A.M. Neto, J.D. Nero, Electron scattering processes in steroid molecules via NEGF-DFT: the opening of conduction channels by central oxygen, J. Mol. Graph. Model. 101 (2020) 107755, http://dx.doi.org/10.1016/j.jmgm.2020.107755.

[47] Jogender, B. Badhani, Mandeep, R. Kakkar, A DFT-D2 study on the adsorption of phosgene derivatives and chloromethyl chloroformate on pristine and Fe4 -decorated graphene, J. Mol. Graph. Model. 101 (2020) 107754, http://dx.doi.org/10.1016/j.jmgm.2020.107754.

[48] A.M. Rodrigues, A.R. Palheta-Junior, M.S.S. Pinheiro, A.M.R. Marinho, A.M.J. Chaves-Neto, R. Gester, T. Andrade-Filho, Encapsulation ability of silicon carbide and boron nitride nanotubes for spilanthol molecule, J. Nanostruct. Chem. 11 (2020) 203, http://dx.doi.org/10.1007/s40097-020-00359-5.